

## Performance of a right-triangle stilling basin: a laboratory investigation

Asma Rabiei<sup>a</sup>, Jahanshir Mohammadzadeh-Habili<sup>a</sup>, Aaron Anil Chadee<sup>b</sup>, Seyed Mohammadali Zomorodian<sup>a</sup>, Mohammed Jameel<sup>c</sup> and Hazi Mohammad Azamathulla <sup>b,\*</sup>

<sup>a</sup> Department of Water Engineering, School of Agriculture, Shiraz University, Shiraz, Iran

<sup>b</sup> Department of Civil and Environmental Engineering, University of the West Indies, St Augustine, Trinidad And Tobago

<sup>c</sup> Department of Civil Engineering, College of Engineering, King Khalid University, Abha, Saudi Arabia

\*Corresponding author. E-mail: azmatheditor@gmail.com

 HMA, 0000-0002-5436-4147

### ABSTRACT

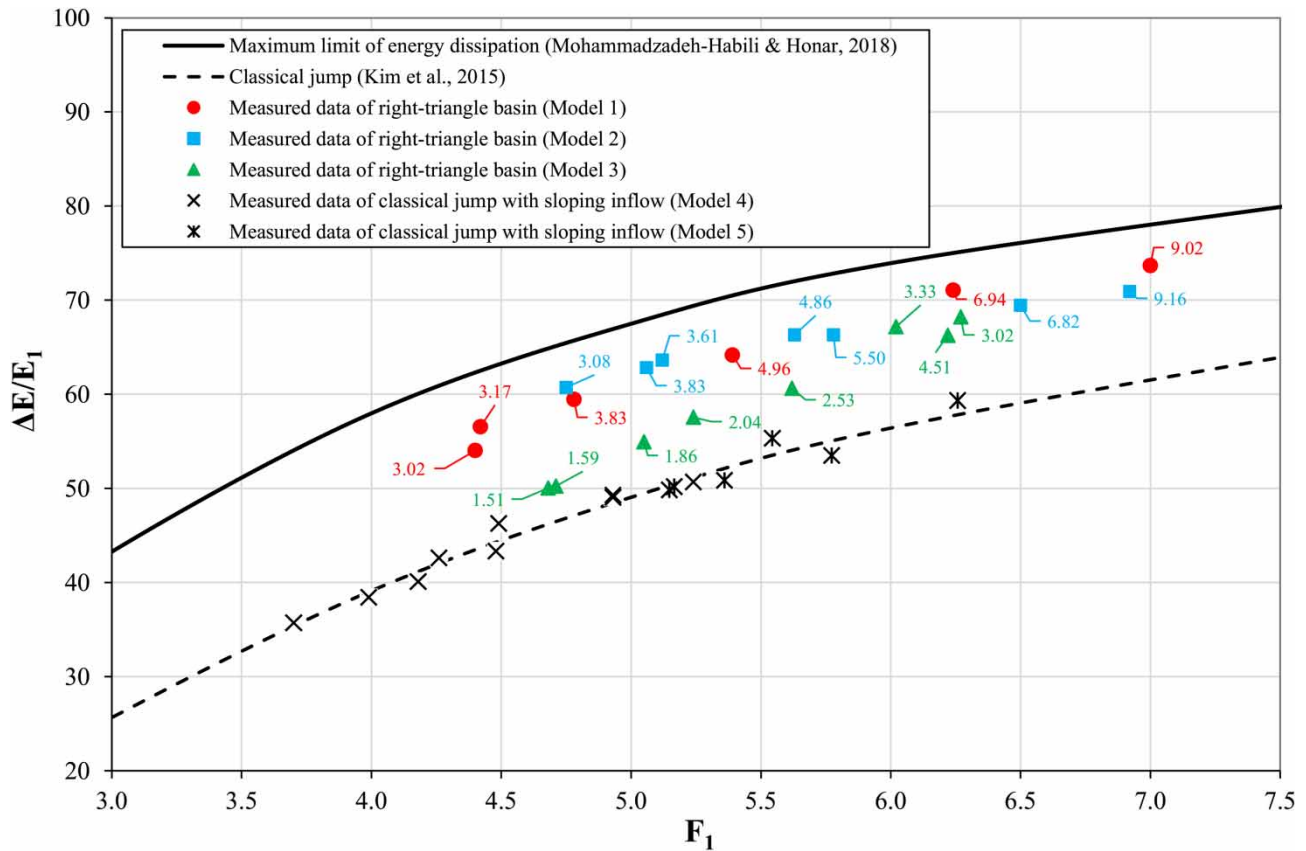
One of the most used hydraulic structures for energy dissipation of supercritical flow is the hydraulic jump stilling basin. From dimensional analysis, the sequent flow depth ratio of a hydraulic jump over the right-triangle basin is derived as a function of the inflow Froude number and relative length of the basin front. The proposed structure stabilized the hydraulic jump at the toe of the chute spillway and hydraulic jump characteristics were investigated for the Froude number ranging from  $4.4 < F_1 < 7$ . The results obtained from both numerical and experimental simulations yielded increased efficiency in the energy dissipation performance of this novel design. The modeling showed the formation of two large recirculation regions at the jump roller and jump bed at the beginning of the downstream channel, which resulted in intense energy dissipation in the right-triangle basin. The relative energy loss is approximately 37% higher for relative basin front lengths larger than three compared to the classic jump. Practitioners and academia on the usefulness of a right-triangle basin for hydraulic purposes and further experimental tests are needed to estimate the scalability and cost-benefit of this modified system for implementation.

**Key words:** chute spillway, energy dissipation, hydraulic jump, right-triangle basin, sequent depth

### HIGHLIGHTS

- The right-triangle basin with the downstream horizontal channel, as a modified energy dissipation structure.
- For this design, the frontal face of the basin is set perpendicular to the inflow direction and its end edge is at the same level as the downstream horizontal channel bed.
- The results obtained from both numerical and experimental simulations efficiency in energy dissipation performance of this novel design.

## GRAPHICAL ABSTRACT



## 1. INTRODUCTION

Hydraulic jump serves as the essential phenomenon to dissipate the excess energy of supercritical flow downstream of the hydraulic structures by its great turbulent mixture over a short length and a rise in flow depth (Henderson 1966). A hydraulic jump formed over a rectangular horizontal channel is known as the classical hydraulic jump (Hager 1992). Based on the Bélanger equation, the sequent depth ratio of classical hydraulic jump is related to the inflow Froude number (Hager 1993):

$$\frac{d_2^*}{d_1} = \frac{1}{2} \left( \sqrt{1 + 8F_1^2} - 1 \right) \quad (1)$$

where  $d_2^*$  is the sequent depth of classical hydraulic jump (m);  $d_1$  is the initial depth of hydraulic jump (m); and  $F_1$  is the inflow Froude number (-).

One must be sure that the hydraulic jump, as an energy dissipater, forms not only during all the possible flow conditions but its position remains constant (Hager & Sinniger 1985). To stabilize the situation of hydraulic jump downstream of hydraulic structures and to increase energy dissipation along hydraulic jump, different energy dissipation structures such as steps, stilling basins have been investigated over the years. A positive step is one of the basic types of stilling basins defined as a local rise in the horizontal channel bottom and the front of step is perpendicular to the flow direction (Hager & Sinniger 1985). Due to stability in jump position, especially on the small Froude numbers, attentions are pointed toward positive step by researchers (Hager & Bretz 1986). For hydraulic jump over a positive step in a horizontal bed, Rajaratnam (1965) stated that the flow rise is noticeable just over the step site and Karki *et al.* (1972) showed that the pressure on the front of the step is greater than the hydrostatic pressure. Applying the momentum equation, Hager & Sinniger (1985) derived theoretical equations for relating the sequent depth ratio of the hydraulic jump over the positive step into the inflow Froude number and relative step height. Four flow regimes over a positive step were experimentally identified by Hager & Bretz (1986). Apart

from these substantial hydraulic studies, the elementary geometry of a positive step as a jump basin has a significant impact on the construction process and therefore the costs of the project. Due to its static stability, an abrupt rise as a stilling basin does not require further structures such as roughened bed, chute blocks (Demetriou & Dimitriou 2010). In recent years, a new theoretical model with great accuracy was developed based on a one-dimensional momentum equation to estimate the conjugate flow depth, jump length and, energy dissipation of hydraulic jump in a horizontal rectangular channel with an abrupt rise (Mohammadi *et al.* 2021; Pandey *et al.* 2023; Zolghadr *et al.* 2023). The important matter of the jump location and its displacement in a sill-controlled jump basin was investigated by Hafnaoui & Debabeche (2023). Meanwhile, Zhou *et al.* (2023) highlighted the obligation on avoiding wave-type flow occurring under no tailwater conditions in channels equipped with abrupt rise.

Despite many studies of hydraulic jump over the positive step in a horizontal bed, the issue of hydraulic jump on sloping beds with positive steps is less addressed. A hydraulic jump over a positive step in an inclined channel can result in high energy losses (Demetriou & Dimitriou 2010). The soil conservation service of the U.S. Department of Agriculture has advised the engineers to construct a channel with a floor slope of 1V:3H for the chute spillway. The hydraulic jump forming on a slope greater than 0.33 (18°) may act differently (Rajaratnam 1963). The jump on the sloping channel was investigated by Quraishi & Al-Brahim (1992), followed by Husain *et al.* (1994) and Negm (1996). Quraishi & Al-Brahim (1992) classified the hydraulic jump over the positive step in a sloping bed into A-jump and B-jump. For the B-jump, an uprising in flow depth is formed over the situation of a positive step, and the jump is formed by decreasing the tailwater depth of an A-jump. Formation of the hydraulic jump under proper topographic situation and tailwater depth on sloping channels results in considerable energy dissipation (Quraishi & Al-Brahim 1992). Several empirical equations are suggested by Husain *et al.* (1994) to estimate the conjugate flow depth and jump length for any jump type at a positive step. A modified Froude number depending on channel slope and step height is then derived by Negm (1996). Nevertheless, the formation of the hydraulic jump on steep slopes is a fundamental concern for engineers (Beirami & Chamani 2006). Working conditions of a positive step as a stilling basin in a steep channel with supercritical downstream flow regimes were examined experimentally by Carravetta & Vacca (2009).

To shed light on the matter of hydraulic jumps on sloping beds, researchers have mostly examined stilling basins with adverse slopes. Bateni & Yazdandoost (2009) used momentum equations and experimental results to drive relations predicting sequent depth ratio and roller length of jump on an adverse sloping floor. Nonetheless, the formation of the hydraulic jump on an adverse slope is still a challenging issue due to the unstable configuration of hydraulic jumps (Parsamehr *et al.* 2017). An experiment conducted by Pourabdollah *et al.* (2020) proved that the adverse slope equipped with a positive step increases energy loss. Results of Mazumder (2022) experiments on several stilling basins with varying adverse slopes combined with a positive step with different heights implied 13% higher energy loss than classical jump. Rising energy loss of the high kinetic energy of flow downstream of hydraulic structures with different methods is a crucial aspect to be considered for designers (Daneshfaraz *et al.* 2023).

To convey flow from high to low elevation efficiently, a chute spillway which requires lower excavation in hilly regions is necessary. For chute spillways, the steep slope of the chute bed is usually terminated by the horizontal bed of downstream channel and energy dissipators are essential elements at the spillway end to mitigate the damaging erosive impacts (Daneshfaraz *et al.* 2021b). Utilizing elements such as fishway on sloping bed can also act as an energy dissipator structure (Daneshfaraz *et al.* 2021a). But due to the development of the Roller Compacted Concrete (RCC) construction technique, stepped chutes have attracted the attention of engineers in recent years. Although United States Bureau of Reclamation (USBR) stilling basins have performed well under the experimental study of a stepped chute spillway (Valero *et al.* 2018; Hunt & Kadavy 2021), stepped chutes require 17% longer stilling basin lengths (Stojnic *et al.* 2022). While numerous investigations have been conducted on energy dissipation of stepped spillways, few have been conducted on energy dissipators for smooth chute spillways.

Given the current global drive for more sustainable structures with smaller carbon footprints and alignment to the United Nations' sustainable development goals (SDGs), optimizing existing standardized designs are ongoing. The present study aims to introduce and investigate the application of a positive step at the intersection of the chute bed with the downstream horizontal channel, named right-triangle basin, as a new energy dissipation structure for dissipating the excess energy of supercritical flow downstream of the chute spillway located in hilly regions. Thus, in terms of scaling the experimental modeling to praxis, vulnerable island nations such as small island developing states (Chadée *et al.* 2021) can immediately benefit from hydraulic energy dissipation structures based primarily on size, cost, and location. Finally, previously, experimental

study provided only at a point or on a plane chance for observation and measurement of the hydraulic jump's parameters. Now the sophisticated nature of jumps can be understood by a Computational Fluid Dynamics (CFD) simulation (De Padova & Mossa 2021). To this end, hydraulic jump properties over the right-triangle basin were investigated by using dimensional analysis, and experimental and numerical simulations.

## 2. MATERIALS AND METHODS

### 2.1. Geometry of right-triangle basins

The right-triangle basin consists of a positive step at the intersection of the chute spillway with the downstream horizontal channel. The longitudinal cross-section of right-triangle basin and hydraulic jump over the basin are schematically plotted in Figure 1.

Returning loose materials from downstream to upstream by backward flows would result in abrasion and destruction of right-triangle basins. This process would be avoided by establishing forward developing flow over the loose materials on downstream of basin. To this end, the length of  $L_d$  should be protected with appropriate materials such reinforced concrete. Constructing the front of basin with reinforced concrete is also advised.

### 2.2. Dimensional analysis

The main variables of hydraulic jump over the right-triangle basin can be linked together by the following functional relationship:

$$\phi(Q, B, d_1, d_2, z, \theta, g, \nu, \rho) = 0 \quad (2)$$

where  $\phi$  is the functional symbol;  $Q$  is the flow discharge ( $\text{m}^3/\text{s}$ );  $B$  is the channel width (m);  $g$  is the acceleration due to the gravity ( $\text{m}/\text{s}^2$ );  $\nu$  is the kinematic viscosity ( $\text{m}^2/\text{s}$ ); and  $\rho$  is the water density ( $\text{kg}/\text{m}^3$ ). Applying the Buckingham  $\Pi$  theorem and considering  $Q$ ,  $d_1$  and  $\rho$  as dimensional independent variables, six dimensionless groups of  $\Pi_1$ ,  $\Pi_2$ ,  $\Pi_3$ ,  $\Pi_4$ ,  $\Pi_5$ , and  $\Pi_6$  were derived for hydraulic jump over right-triangle basin as:

$$\Pi_1 = \frac{d_2}{d_1}, \quad \Pi_2 = \frac{z}{d_1}, \quad \Pi_3 = \frac{B}{d_1}, \quad \Pi_4 = \frac{gd_1^5}{Q^2}, \quad \Pi_5 = \frac{\nu d_1}{Q}, \quad \text{and} \quad \Pi_6 = \theta \quad (3)$$

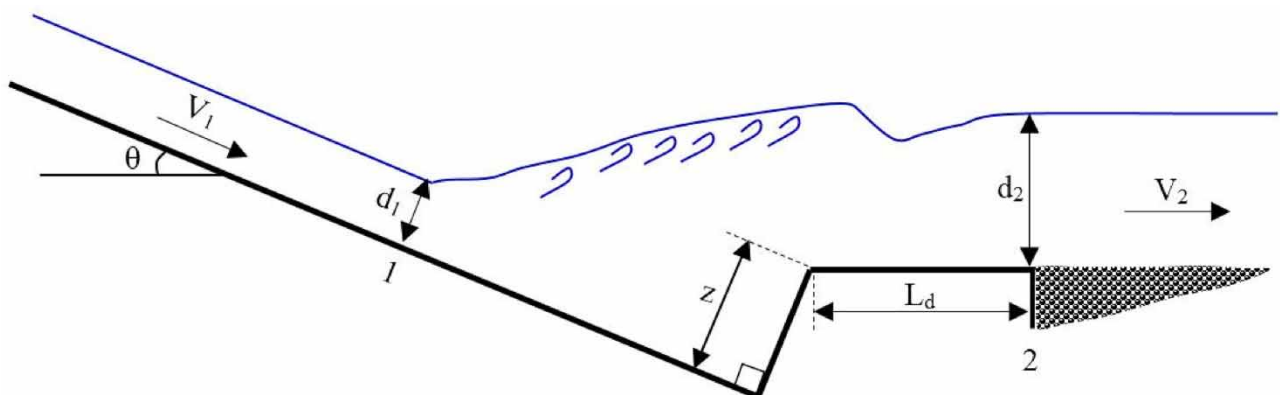


**Figure 1** | Longitudinal cross-section of right-triangle basin and hydraulic jump over the basin,  $z$  is the length of the basin front (m);  $\theta$  is the slope angle of chute spillway ( $^\circ$ );  $d_1$  is the initial depth of hydraulic jump (m),  $d_2$  is the sequent depth of hydraulic jump (m);  $V_1$  is the mean velocity at section 1 (m/s);  $V_2$  is the mean velocity at section 2 (m/s); and  $L_d$  is the required length for establishing developed flow on downstream of basin (m).

To derive the commonly used dimensionless variables in hydraulics, some dimensionless groups should be combined. After combination, dimensionless groups of Equation (3) are related together as:

$$\Pi_1 = f\left(\frac{1}{\Pi_3\sqrt{\Pi_4}}, \Pi_2, \Pi_6, \frac{1}{\Pi_5}, \frac{1}{\Pi_3\Pi_5}\right) \quad (4)$$

Substituting  $\Pi_1, \Pi_2, \Pi_3, \Pi_4, \Pi_5,$  and  $\Pi_6$  from Equation (3) into Equation (4) and considering  $V_1 = Q/Bd_1$  gives:

$$\frac{d_2}{d_1} = f\left(\frac{V_1}{\sqrt{gd_1}}, \frac{z}{d_1}, \theta, \frac{d_1}{B}, \frac{V_1d_1}{\nu}\right) = f\left(F_1, \frac{z}{d_1}, \theta, \omega, Re_1\right) \quad (5)$$

where  $Re_1$  is the inflow Reynolds number (-) and  $\omega$  is the inflow aspect ratio (-).

In the experimental studies of hydraulic jump, the scale effects originate from water viscosity and channel width and result in deviations between the model and prototype observations (Hager & Bremen 1989). Based on Hager & Bremen (1989), a hydraulic jump is not influenced by scale effects if  $\omega < \omega_L$ , where  $\omega_L$  is the limit value for scale effects and is the function of  $F_1$  and  $Re_1$  as:

$$\omega_L = \frac{1 - 14(\log Re_1)^{-2.5} \exp(F_1/8)}{65[(\log Re_1)^{-3} \exp(F_1/7) - 0.7(\log Re_1)^{-5.5} \exp(F_1/3.73)]} \quad (6)$$

Furthermore, the same procedure of analysis results in the following relation between the relative energy loss with dimensionless variables:

$$\frac{\Delta E}{E_1} = f\left(\frac{V_1}{\sqrt{gd_1}}, \frac{z}{d_1}, \theta, \frac{d_1}{B}, \frac{V_1d_1}{\nu}\right) = f\left(F_1, \frac{z}{d_1}, \theta, \omega, Re_1\right) \quad (7)$$

### 2.3. Experimental and numerical setup

Experiments of the present study were performed out in a 11 m long rectangular horizontal flume, internally 0.40 m wide and 0.60 m high in cross section. The flume sidewalls and its floor were constructed of glossy and smooth stone sheets with minimal surface roughness. To simulate the hydraulic jump over the right-triangle basin, two chute spillways with height ( $P$ ) of 39.6 and 54.0 cm and two different lengths of the basin front ( $z$ ) of 6 and 12 cm were made of transparent Plexiglas plates and installed in the flume (Figure 2). To reduce head loss over the chute crest surface and obtain a smooth flow over the downstream surface of the chute models, a semicircular PVC pipe with a diameter of 20 cm was embedded at the entrance of the chute models. Based on the advised and applied slope for chute bed in some practical projects (Bakhmeteff & Matzke 1938; Rajaratnam 1963; Michels 1977), downstream surface of chute spillway models was installed at the slope angle of  $\theta = 18.43^\circ$  or  $\tan\theta = (1/3)$ . To diminish the water surface fluctuation and consequently, to reach horizontal water surface profile above the chute models, a stilling tank following by several sequential grid pages were placed above the site of chute models. For installation of right-triangle basin models, the flume bed on downstream of chute models was 11.4 cm elevated by using the Plexiglas plates. For measurement of longitudinal pressure distribution over the bed of hydraulic jump, seven piezometers were embedded under the downstream part of the chute floor, basin front, and downstream flume bed. Piezometers were then connected to a piezometer board, installed beside of the flume wall.

In this study, ANSYS FLUENT software was applied to generate the computational mesh on the 3D simulated model of the right-triangle basin by AUTOCAD. Solution of the Navier Stokes equations is the basis of ANSYS FLUENT software package. These equations are based on mass and momentum flux balances. Meanwhile, only 4 m length of the channel is simulated to decrease computing time. A triangular unstructured mesh is selected in this study for computation. To determine the free surface of flow, a VOF model is utilized and for the numerical simulation the  $k-\varepsilon$  turbulence model is used. Boundary conditions include the air and water inlet for entrance section, pressure for outlet section, walls for bed and sides of the channel and pressure boundary for free surface of the flow. The Average Relative Error (ARE) criterion is used to evaluate the consistency between the numerical and experimental models. The mesh study analysis corresponding to the simulation of

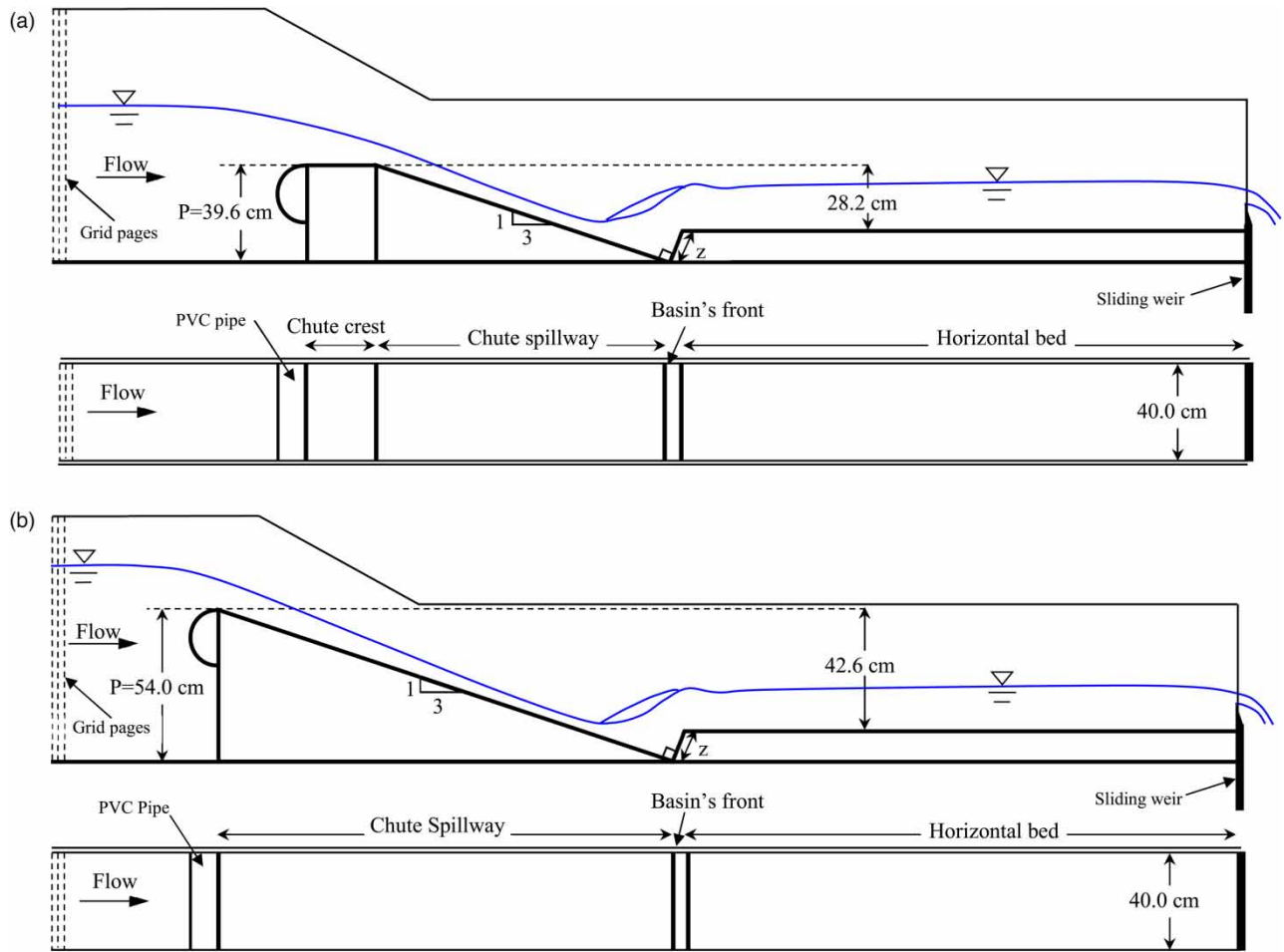


**Figure 2** | Longitudinal cross-section and plan view of the experimental setups: (a) model 1 ( $P = 39.6$  cm,  $z = 12$  cm) and (b) models 2 and 3 ( $P = 54$  cm,  $z = 6$  or  $12$  cm).

a test with  $Q = 0.0410$  m<sup>3</sup>/s,  $z/d_1 = 3.17$ , and  $F_1 = 4.42$  resulted in 1189524 number of nodes. The error analysis, which is based on the comparison of experimental water surface with numerical results, showed a value about 5.55% for the Average Relative Error (ARE).

#### 2.4. Model operation

The water flow system in the flume was recirculated and flow discharge was regulated using a butterfly valve situated on the transferring water pipe between the pump and flume entrance. Discharge values were measured using the volumetric method. Measurement of flow depth was conducted at the centerline of the flume using a point gauge with  $\pm 0.05$  mm reading accuracy. The minimum required tailwater depth for establishing the hydraulic jump over the right-triangle basin was adjusted with a sliding rectangular sharp-crested weir installed at the flume outlet.

#### 2.5. Flow conditions

Regarding the classification for hydraulic jump on sloping channels with positive or negative step [Quraishi & Al-Brahim \(1992\)](#) introduced two types of jumps known as A-jump and B-jump. Based on described flow condition by [Quraishi & Al-Brahim \(1992\)](#) and measured water surface in this study, the B-jump was formed in experiments. Hydraulic jump characteristics over three models of right-triangle basin (models 1 through 3) were measured. Due to the high turbulence in the jump, flow depth and bed pressure were highly fluctuated, as well as on basin front. Therefore, flow depth and bed pressure were quantified by time-averaged method. To indicate the efficiency of hydraulic jump over the right-triangle basin, some A-jumps on sloping bed without a downstream step was also tested for models 4 and 5 by establishing the initial supercritical depth of



jump at the toe of chute models. Summary of flow conditions and bed geometry of tested hydraulic jumps are presented in Table 1.

### 3. RESULTS AND DISCUSSIONS

For each of the conducted tests, as observed from Table 1, the inflow aspect ratio ( $\omega$ ) is smaller than its corresponding limit value for scale effects ( $\omega_L$ ). Therefore, influences of scale effects and consequently,  $Re_1$  and  $\omega$  on results of present study can be ignored. As a result, the obtained relation for sequent depth ratio of hydraulic jump over right-triangle basin with inlet slope of  $\theta = 18.43^\circ$  (Equation (5)) can be expressed as:

$$\frac{d_2}{d_1} = F\left(F_1, \frac{z}{d_1}\right) \tag{8}$$

Equation (8) indicates that  $F_1$  and  $z/d_1$  are dimensionless influencing parameters on the sequent depth ratio of hydraulic jump over right-triangle basin.

**Table 1** | Summary of flow conditions and bed geometry of tested hydraulic jumps

Model	z (cm)	P (cm)	Q (m <sup>3</sup> /s)	d <sub>1</sub> (cm)	F <sub>1</sub> (-)	Re <sub>1</sub> (-)	d <sub>2</sub> (cm)	L <sub>d</sub> (cm)	ΔE/E <sub>1</sub> (%)	ω (-)	ω <sub>L</sub> (-)
1	12.0	39.6	0.04386	3.98	4.4	109,650	17.58	76	54.03	0.10	0.61
			0.04099	3.79	4.42	102,475	15.58	56	56.55	0.09	0.59
			0.03316	3.13	4.78	82,900	13.95	51	59.46	0.08	0.49
			0.02542	2.42	5.39	63,550	12.03	51	64.20	0.06	0.36
			0.01774	1.73	6.24	44,350	8.98	41	71.07	0.04	0.22
			0.01342	1.33	7	33,550	8.01	26	73.69	0.03	0.12
2	12.0	54.0	0.04572	3.89	4.75	114,300	16.3	60	60.72	0.10	0.57
			0.03885	3.32	5.12	97,125	14.9	56	63.62	0.08	0.48
			0.03514	3.13	5.06	87,850	14.1	50	62.82	0.08	0.47
			0.02736	2.47	5.63	68,400	12.5	45	66.31	0.06	0.35
			0.02338	2.18	5.78	58,450	11.8	41	66.31	0.05	0.31
			0.01894	1.76	6.5	47,350	10.9	28	69.45	0.04	0.21
			0.01299	1.31	6.92	32,475	8.8	21	70.91	0.03	0.12
3	6.0	54.0	0.04664	3.98	4.68	116,600	22.4	78	50.05	0.10	0.58
			0.04361	3.77	4.71	109,025	21.5	73	50.23	0.09	0.56
			0.03669	3.23	5.05	91,725	18.8	65	54.94	0.08	0.48
			0.03312	2.94	5.24	82,800	17.2	56	57.57	0.07	0.43
			0.02572	2.37	5.62	64,300	14.7	47	60.63	0.06	0.34
			0.0221	1.99	6.27	55,250	12	40	68.22	0.05	0.25
			0.01825	1.8	6.02	45,625	10.3	33	67.18	0.05	0.24
			0.01194	1.33	6.22	29,850	8.5	23	66.26	0.03	0.16
4	0.0	39.6	0.05183	5	3.7	129,575	23.7	-	35.70	0.13	0.76
			0.04191	4	4.18	104,775	22.2	-	40.11	0.10	0.63
			0.03706	3.8	3.99	92,650	19.9	-	38.41	0.10	0.62
			0.03344	3.4	4.26	83,600	18.6	-	42.63	0.09	0.56
			0.02922	3	4.49	73,050	16.9	-	46.28	0.08	0.50
			0.02351	2.6	4.48	58,775	15.5	-	43.32	0.07	0.45
			0.02017	2.2	4.93	50,425	14.1	-	49.07	0.06	0.37
			0.01881	2.1	4.93	47,025	13.4	-	49.28	0.05	0.35
			0.01089	1.4	5.24	27,225	9.8	-	50.68	0.04	0.22
5	0.0	54.0	0.04777	3.8	5.15	119,418	26.1	-	49.82	0.10	0.53
			0.04421	3.6	5.17	110,523	24.7	-	50.19	0.09	0.51
			0.03791	3.1	5.54	94,779	21.7	-	55.32	0.08	0.43
			0.02654	2.5	5.36	66,357	18.2	-	50.85	0.06	0.38
			0.01894	1.9	5.77	47,352	15.1	-	53.51	0.05	0.27
			0.01299	1.4	6.26	32,467	11.3	-	59.32	0.04	0.17

In Figure 3, the measured sequent depth ratio data of tested hydraulic jumps is shown against inflow Froude number. The relative step height ( $z/d_1$ ) value for each tested hydraulic jump over right-triangle basin models is also added as a label for jump data points. For comparison of results, the curve of Bélanger equation (Equation (1)), classical jump data with horizontal supercritical approach flow (Hager & Bremen 1989), and data of hydraulic jump over USBR type III stilling basin (Frizell et al. 2012) are added in Figure 3.

It follows from Figure 3 that the sequent depth ratio of hydraulic jump over right-triangle basin is increased with increasing inflow Froude number. For  $z/d_1 < 3$ , increasing in relative basin front length resulted in reduction in sequent depth ratio of hydraulic jump over right-triangle basin. But after that ( $3 < z/d_1$ ), more reduction in  $d_2/d_1$  is not nearly achieved by increasing in  $z/d_1$ . Therefore, to achieve the smallest required sequent depth for hydraulic jump over right-triangle basin, the relative step height range of  $3 < z/d_1$  is advised for design of right-triangle basin. For  $3 < z/d_1$ , sequent depth ratio of hydraulic jump over right-triangle basin is averagely obtained 30% smaller than that of the classical jump. It is also obtained 15% smaller than that of hydraulic jump data over USBR type III stilling basin, indicating usefulness of right-triangle basin for practical purposes.

To estimate the sequent depth ratio of hydraulic jump over right-triangle basin with inlet slope of  $\theta = 18.43^\circ$  from  $F_1$  and  $z/d_1$ , the multi-variable regression was applied, and the following equation is accurately fitted to experimentally measured data of hydraulic jump over the right-triangle basin models:

$$\frac{d_2}{d_1} = 0.767(F_1)^{1.309} \left(\frac{z}{d_1}\right)^{-0.214} \tag{9}$$

The Mean Absolute Percentage Error (MAPE) of Equation (9) for estimating the sequent depth ratio of hydraulic jump over right-triangle basin models was calculated as 5.3%, indicating high accuracy of the developed equation.

For three tests of conducted hydraulic jumps over right-triangle basin models, the longitudinal measured profiles of water surface and bed pressure are plotted in Figure 4. It can be resulted that the incoming jet into the right-triangle basin created a

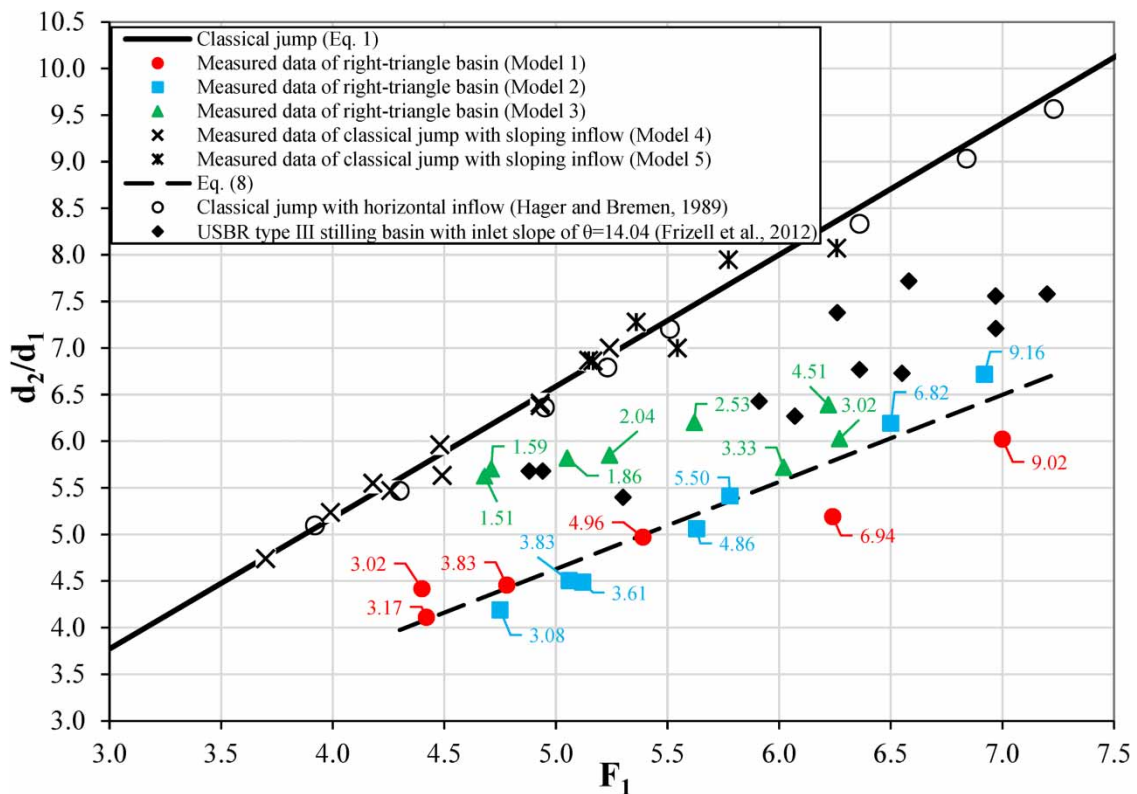


**Figure 3** | Measured sequent depth ratio data ( $d_2/d_1$ ) versus  $F_1$  of hydraulic jump over right-triangle basin compared to classical hydraulic jump and hydraulic jump over USBR type III stilling basin. Numbers above each data refers to its corresponding  $z/d_1$ .



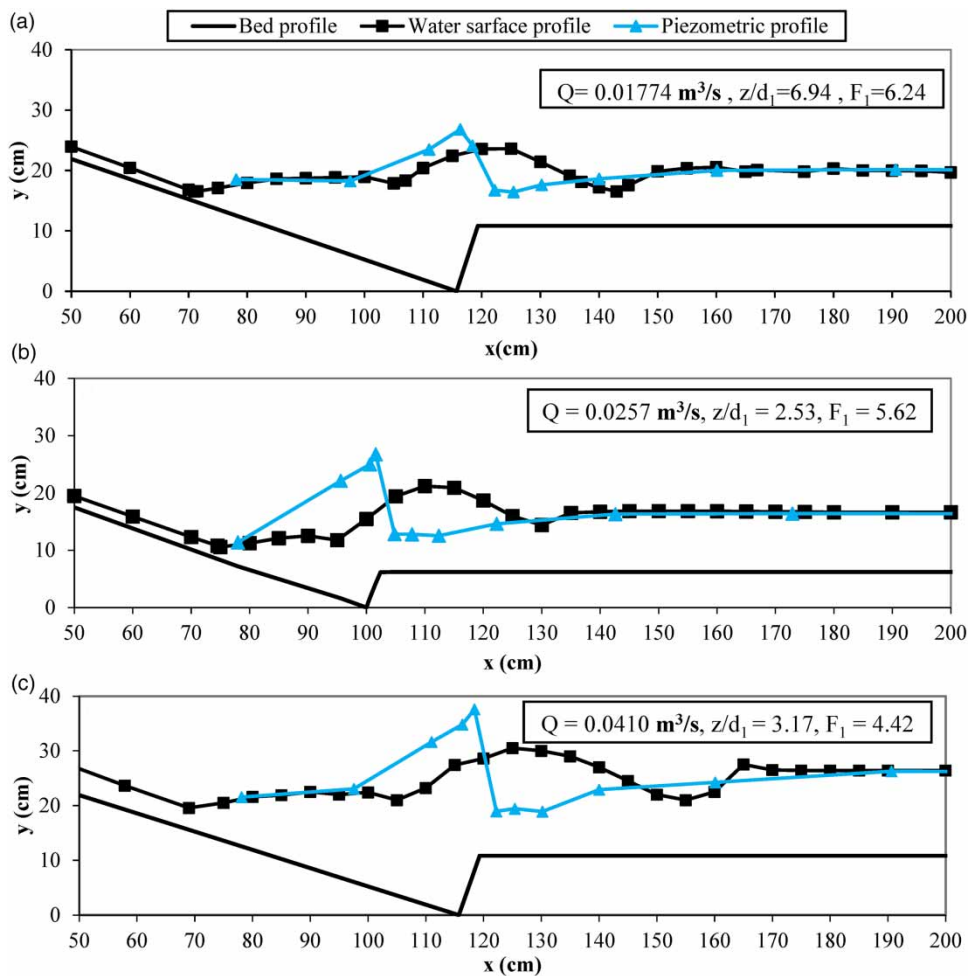


**Figure 4** | The longitudinal measured profiles of water surface and bed pressure of three tested hydraulic jump over right-triangle basin: (a) model 1, (b) model 3, and (c) model 1.

stagnation pressure at the basin front, resulting in surplus pressure and consequently, uniform, and non-hydrostatic pressure distribution over the basin front. Due to inclined-upward direction of flow over the basin front, water flow separated from the basin front and then reattached to the downstream horizontal bed surface. This process resulted in developing of a flow-separation zone with recirculation flow and a flow-depth rising zone over the basin front. Placing the piezometric pressure profile below the water surface profile at beginning portion of downstream channel validates the formation of a separation zone just after the basin front. As negative or sub-atmospheric pressure had not occurred in the separation zone, downstream of the right-triangle basin would not be subjected to cavitation danger. After the apex of flow-depth rising zone, the flow depth is decreased due to reattachment of separated flow to the horizontal channel bed. Then, the flow depth is smoothly increased and reached to the tailwater depth. In the following, water surface and bed pressure profiles are matched together, indicating developing flow.

Regarding the jump type classification, A-jump has been described as a jump that entirely located at upstream zone of an abrupt rise over a sloping bed. It means that the termination section of its roller length is exactly at the starting point of the positive rise (Quraishi & Al-Brahim 1992). However, B-jump is characterized by its roller length location which is partly upstream and partly downstream of an abrupt rise and decreasing the tailwater in B-jump results in two distinct portions for roller length (Quraishi & Al-Brahim 1992). Assessment of jump type based on the comparison of Quraishi & Al-Brahim (1992) classifications and longitudinal profile of water surface in this study (Figure 4) substantiates the formation of B-jump over right-triangle basin.

Figure 5 displays the relative energy dissipation  $\Delta E/E_1$  of tested hydraulic jumps against inflow Froude number  $F_1$ . For comparison of results, the curves of relative energy dissipation of classical hydraulic jump from Kim *et al.* (2015) and maximum limit of energy dissipation from Mohammadzadeh-Habili & Honar (2018) are plotted in Figure 5. Based on Mohammadzadeh-Habili *et al.* (2018), the maximum limit of energy dissipation is achieved if the sequent depth of hydraulic jump is equal to critical flow depth.

As it can be observed from Figure 5, energy dissipation of hydraulic jump over right-triangle basin is significantly larger than that of the classical hydraulic jumps with horizontal and sloping inflows. For  $3 < z/d_1$ , the relative energy dissipation data of hydraulic jumps over right-triangle basin is very close to the maximum limit of energy dissipation curve, indicating intense energy dissipation that resulted in smaller sequent depth of hydraulic jump over right-triangle basin compared to classical hydraulic jump, as previously observed from Figure 3. Relative energy loss increased with rise in  $z/d_1$  of the right-triangle basin by 37% compared to classical jump on horizontal floor downstream of chute.

To indicate the impact of right-triangle basin on flow dynamics and energy loss, the CFD technique was used and flow pattern over the right-triangle basin is numerically simulated by ANSYS FLUENT software package for a test with  $Q = 0.0410 \text{ m}^3/\text{s}$ ,  $z/d_1 = 3.17$ , and  $F_1 = 4.42$  (Figure 6). As it can be seen from Figure 6(a), simulated water surface profile over the right-triangle basin is like that of experimentally measured in Figure 4(c). Additionally, two large recirculation regions were formed along the hydraulic jump over right-triangle basin. First recirculation region was formed over the jump roller and the second was formed over the jump bed at beginning of the downstream horizontal channel (Figure 6(b)). Formation of the second recirculation zone was previously resulted from measured profiles of water surface and bed pressure in Figure 4. As recirculation regions are sources for energy loss (Ramamurthy *et al.* 1998; Mohammadzadeh-Habili *et al.* 2013, 2016), intense energy loss in hydraulic jump over the right-triangle basin can be attributed to formation of two large recirculation regions over the roller and bed of jump. Previous research has also pointed out the significance of a bottom vortex downstream of the abrupt rise on stabilizing the jump while amplifying the energy losses (Carravetta & Vacca 2009).

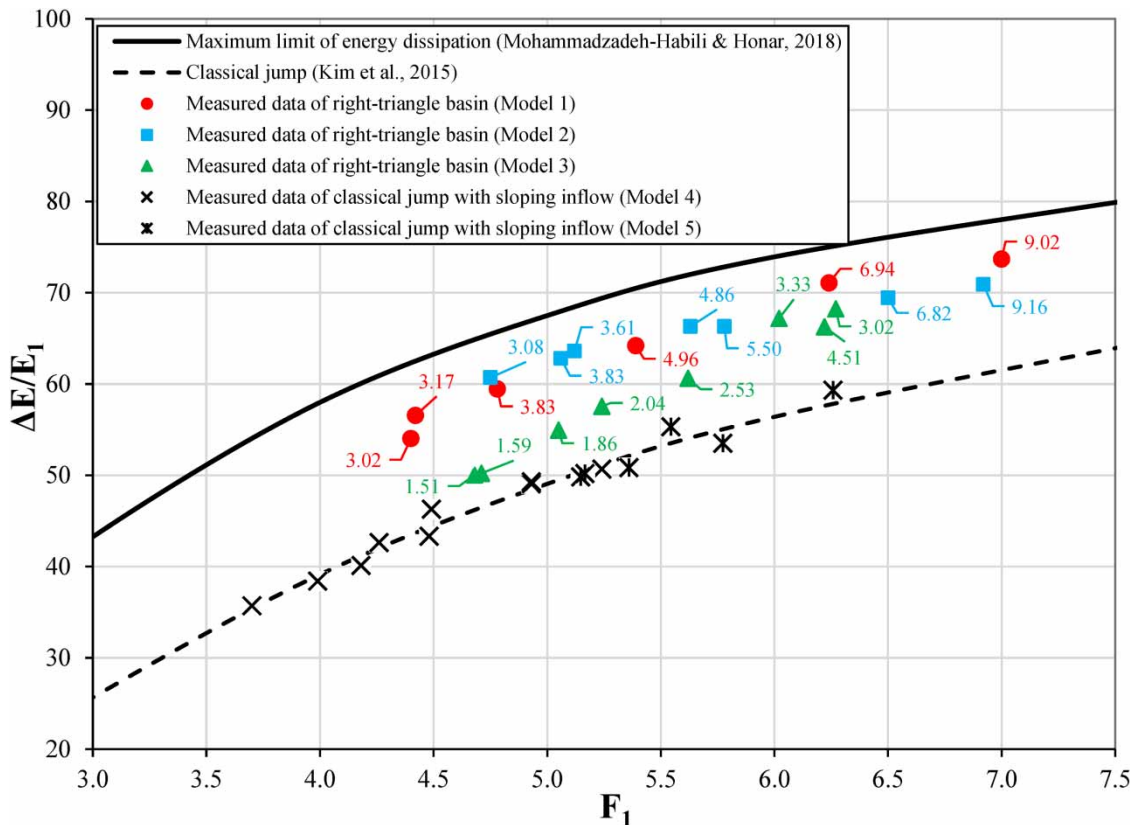
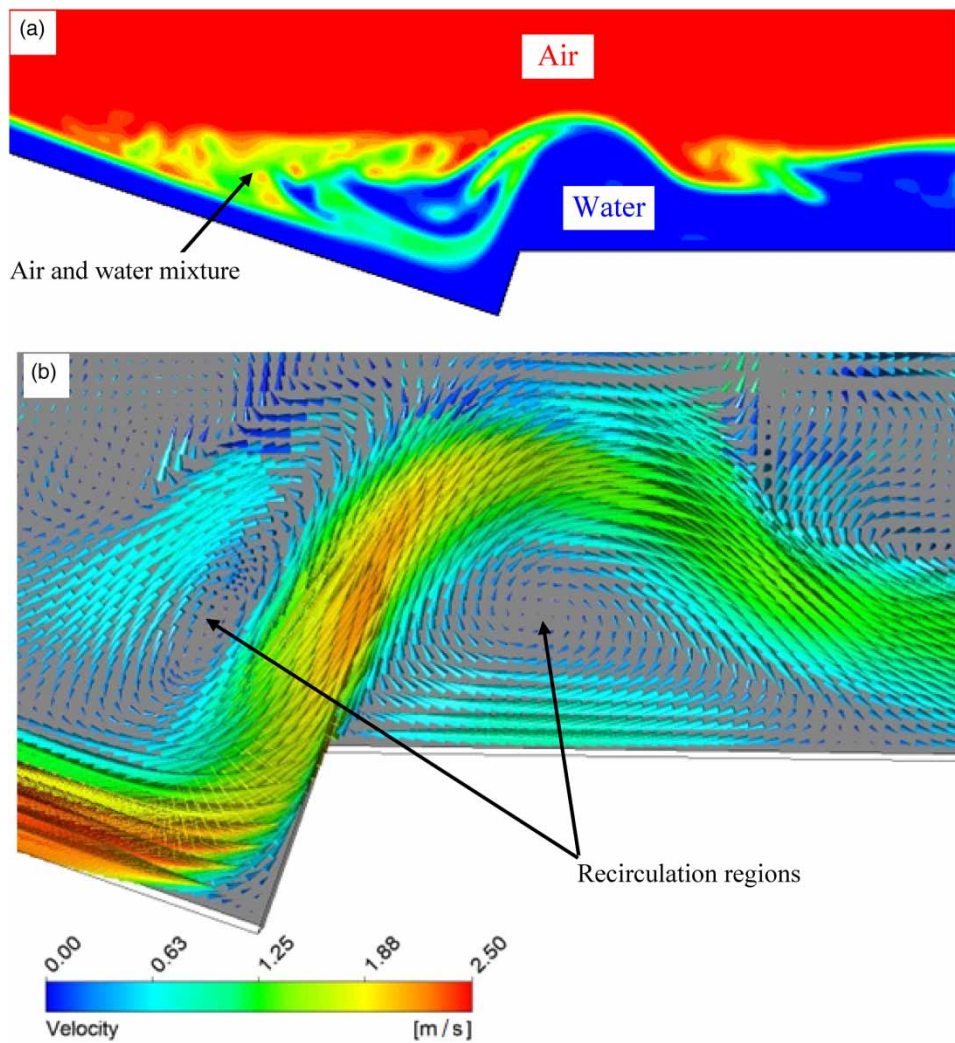


Figure 5 | Energy dissipation ( $\Delta E/E_1$ ) versus  $F_1$  of hydraulic jump over right-triangle basin compared to classical hydraulic jump and maximum limit of energy dissipation. Numbers above each data refers to its corresponding  $z/d_1$ .



**Figure 6** | Numerical simulation of hydraulic jump over right-triangle basin: (a) water surface profile of hydraulic jump and (b) velocity vectors along hydraulic jump.

As previously observed from Figure 4, the downstream flow of hydraulic jump over the right-triangle basin is not immediately developed just after the basin front. Although this experiment was conducted on non-erosive bed material, it is strongly suggested to construct the length of  $L_d$  with reinforced concrete for fulfilling the safety criteria of the structure. To estimate the required length for developing flow on downstream of hydraulic jump over the right-triangle basin, the dimensional analysis was first applied similar to that of applied for sequent depth ratio of hydraulic jump. Then, by neglecting the effect of scale effects and applying the multi-variable regression, the following relation was developed for estimation of  $L_d$  as:

$$\frac{L_d}{d_2} = 9.785(F_1)^{0.515} \left( \frac{z}{d_1} \right)^{-1.168} \quad (10)$$

The MAPE of Equation (10) for estimation of  $L_d/d_2$  was calculated as 10.5%, indicating acceptable accuracy of the developed equation.

#### 4. CONCLUSIONS

This study introduced a new conceptual model of a right-triangle basin to dissipate the excess energy of supercritical flow on downstream of chute spillway. In comparison to the classical hydraulic jump models, energy dissipation of hydraulic jump

over right-triangle basin is significantly larger. The formation of two large recirculation regions over both the jump roller and jump bed at beginning of the downstream horizontal channel is the main reason for large energy dissipation. Due to this larger energy dissipation, a smaller tailwater depth is required for stabilizing hydraulic jump in the proposed stilling basin design.

To achieve the smallest required sequent depth for hydraulic jump over right-triangle basin, the range of the relative basin front length of  $3 < z/d_1$  is advised for design optimality of the right-triangle stilling basin. However, the results of this study and suggested relationships are applicable for tested hydraulic jumps over right-triangle basin under geometric and hydraulic conditions of  $\theta = 18.43^\circ$ ,  $4.4 < F_1 < 7.0$ , and  $z/d_1 < 9.2$ . This design achieves an increased energy loss of approximately 37% as compared to classical jump on horizontal floor downstream of chute. Thus, this design can provide an improved and efficient energy dissipator in stilling basin construction and allow for a less maintenance issues due to erosion and scour during the lifecycle of the structure.

To practically implement this design, contemporary construction practices will have to be modified to accommodate extra excavation and concrete works to position the right-triangle basin, which is the downstream of chute spillway. It is also envisaged that the structure of right-triangle basin could act as an end sill at the toe of chute and, consequently, reduce the discharge seepage from the chute foundation. This is the subject for future studies to justify the economics and sustainability of the right-triangle basin for practical applications.

## ACKNOWLEDGEMENTS

The authors extend their appreciation to the deanship of scientific research at King Khalid University for funding this work through large group research project under grant number (RGP2/94/44).

## DATA AVAILABILITY STATEMENT

All relevant data are included in the paper or its Supplementary Information.

## CONFLICT OF INTEREST

The authors declare there is no conflict.

## REFERENCES

- Bakhmeteff, B. A. & Matzke, A. E. 1938 The hydraulic jump in sloped channels. *Transactions of the American Society of Mechanical Engineers* **60**, 111–118.
- Bateni, S. M. & Yazdandoost, F. 2009 Hydraulics of B-F and F jumps in adverse-slope stilling basins. *Water Management* **162** (5), 321–327.
- Beirami, M. K. & Chamani, M. R. 2006 Hydraulic jumps in sloping channels: sequent depth ratio. *Journal of Hydraulic Engineering* **132** (10), 1061–1068.
- Carravetta, A. & Vacca, A. 2009 Hydraulic design of stilling basins in steep channels. *Dam Engineering* **19** (4), 257.
- Chadee, A. A., Ray, I. & Chadee, X. T. 2021 Systemic issues influencing technical certainty in social housing programmes in a small island developing state. *Buildings* **11** (2), 65.
- Daneshfaraz, R., Aminvash, E., Bagherzadeh, M., Ghaderi, A., Kuriqi, A., Najibi, A. & Ricardo, A. M. 2021a Laboratory investigation of hydraulic parameters on inclined drop equipped with fishway elements. *Symmetry* **13**, 1643.
- Daneshfaraz, R., Aminvash, E., Ghaderi, A., Abraham, J. & Bagherzadeh, M. 2021b SVM performance for predicting the effect of horizontal screen diameters on the hydraulic parameters of a vertical drop. *Applied Science* **11** (9), 4238.
- Daneshfaraz, R., Norouzi, R., Ebadzadeh, P., Di Francesco, S. & Abraham, J. P. 2023 Experimental study of geometric shape and size of sill effects on the hydraulic performance of sluice gates. *Water* **15**, 314.
- Demetriou, J. D. & Dimitriou, D. J. 2010 A mechanical energy losses comparison in inclined hydraulic jumps over a thin wall and a step. *Journal of Hydrodynamics, Ser. B* **22** (5, Supplement 1), 687–691.
- De Padova, D. & Mossa, M. 2021 Hydraulic jump: a brief history and research challenges. *Water* **13**, 1733.
- Frizell, K. W., Connie, D. & Svoboda, P. E. 2012 *Performance of Type III Stilling Basins – Stepped Spillway Studies*. United States Dept. of the Interior, Bureau of Reclamation, HL-2012-02, Denver, Colorado.
- Hafnaoui, M. A. & Debabeche, M. 2023 Displacement of a hydraulic jump in a rectangular channel: experimental study. *Iranian Journal of Science and Technology, Transactions of Civil Engineering* **47**, 1181–1188.
- Hager, W. H. 1992 *Energy Dissipators and Hydraulic Jump*. Springer, Netherlands.
- Hager, W. H. 1993 Classical hydraulic jump: free-surface-profile. *Canadian Journal of Civil Engineering* **20** (3), 536–539.
- Hager, W. H. & Bremen, R. 1989 Classical hydraulic jump: sequent depths. *Journal of Hydraulic Research* **27** (5), 565–558.
- Hager, W. H. & Bretz, N. V. 1986 Hydraulic jumps at positive and negative steps. *Journal of Hydraulic Research* **24** (4), 237–253.



- Hager, W. H. & Sinniger, R. 1985 Flow characteristics of the hydraulic jump in a stilling basin with an abrupt bottom rise. *Journal of Hydraulic Research* **23** (2), 101–113.
- Henderson, F. M. 1966 *Open Channel Flow*. Macmillan Publishing Co. Inc, New York.
- Hunt, S. L. & Kadavy, K. C. 2021 Types I, II, III, and IV stilling basin performance for stepped chutes applied to embankment dams. *Journal of Hydraulic Engineering* **147** (6), 06021004.
- Husain, D., Alhamid, A. A. & Negm, A. A. M. 1994 Length and depth of hydraulic jumps on sloping floors. *Journal of Hydraulic Research* **32** (6), 899–910.
- Karki, K. S., Chander, S. & Malhotra, R. C. 1972 Supercritical flow over sills at incipient jump conditions. *Journal of Hydraulics Division* **98** (10), 1753–1764.
- Kim, Y., Choi, G., Park, H. & Byeon, S. 2015 Hydraulic jump and energy dissipation with sluice gate. *Water* **7** (9), 5115–5133.
- Mazumder, S. K. 2022 Hydraulic jump control using stilling basin with adverse slope and positive step. *ISH Journal of Hydraulic Engineering* **28** (1), 18–20.
- Michels, V. 1977 Uncontrolled chute spillway with unlined cascade, Dartmouth dam. In *61th Australian Hydraulics and Fluid Mechanics Conference*, Adelaide, Australia.
- Mohammadi, M., Nazari-Sharabian, M. & Karakouzian, M. 2021 A novel analytical method for evaluating the characteristics of hydraulic jump at a positive step. *Water* **13**, 2005.
- Mohammadzadeh-Habili, J. & Honar, T. 2018 Theoretical solution for analysis and design of hydraulic jump on corrugated bed. *Water SA* **44** (4), 647–652.
- Mohammadzadeh-Habili, J., Heidarpour, M. & Afzalimehr, H. 2013 Hydraulic characteristics of a new weir entitled of quarter-circular crested weir. *Flow Measurement and Instrumentation* **33**, 168–178.
- Mohammadzadeh-Habili, J., Heidarpour, M. & Haghiabi, A. 2016 Comparison the hydraulic characteristics of finite crest length weir with quarter-circular crested weir. *Flow Measurement and Instrumentation* **52**, 77–82.
- Mohammadzadeh-Habili, J., Heidarpour, M. & Samiee, S. 2018 Study of energy dissipation and downstream flow regime of labyrinth weirs. *Iranian Journal of Science and Technology, Transactions of Civil Engineering* **42**, 111–119.
- Negm, A. A. M. 1996 Hydraulic jumps at positive and negative steps on sloping floors. *Journal of Hydraulic Research* **34** (3), 409–420.
- Pandey, P., Mishra, A. R., Verma, P. K., Tripathi, R. P., 2023 Study and implementation of smart water supply management model for water drain region in India. In: *VLSI, Microwave and Wireless Technologies. Lecture Notes in Electrical Engineering*, Vol. 877. (Mishra, B. & Tiwari, M., eds). Springer, Singapore.
- Parsamehr, P., Farsadizadeh, D., Hosseinzadeh Dalir, A., Abbaspour, A. & Nasr Esfahani, M. J. 2017 Characteristics of hydraulic jump on rough bed with adverse slope. *ISH Journal of Hydraulic Engineering* **23** (3), 301–307.
- Pourabdollah, N., Heidarpour, M., Abedi-Koupai, J. & Mohamadzadeh-Habili, J. 2020 Hydraulic jump control using stilling basin with adverse slope and positive step. *ISH Journal of Hydraulic Engineering* **28** (1), 10–17.
- Quraishi, A. A. & Al-Brahim, A. M. 1992 Hydraulic jump in sloping channel with positive or negative step. *Journal of Hydraulic Research* **30** (6), 769–782.
- Rajaratnam, N. 1963 The submerged hydraulic jump. *Journal of Hydraulics Division* **89** (1), 139–162.
- Rajaratnam, N. 1965 The hydraulic jump as wall jet. *Journal of Hydraulics Division* **91** (5), 107–132.
- Ramamurthy, A. S., Tim, U. S. & Rao, M. V. 1998 Characteristics of square-edged and round-nosed broad-crested weirs. *Journal of Irrigation and Drainage Engineering* **114** (1), 61–73.
- Stojnic, I., Pfister, M., Matos, J. & Schleiss, A. J. 2022 Plain stilling basin performance below 30° and 50° inclined smooth and stepped chutes. *Water* **14**, 3976.
- Valero, D., Bung, D. B. & Crookston, B. M. 2018 Energy dissipation of a type III basin under design and adverse conditions for stepped and smooth spillways. *Journal of Hydraulic Engineering* **144** (7), 04018036.
- Zhou, Y., Wu, J., Zhao, H., Hu, J. & Bai, F. 2023 Hydraulic performance of wave-type flow at a sill-controlled stilling basin. *Applied Sciences* **13**, 5053.
- Zolghadr, M., Zomorodian, S. M. A., Fathi, A., Tripathi, R. P., Jafari, N. & Mehta, D. 2023 Experimental study on the optimum installation depth and dimensions of roughening elements on abutment as scour countermeasures. *Fluids* **8** (6), 175.

First received 1 June 2023; accepted in revised form 1 August 2023. Available online 12 August 2023